universe

MDPI

Article

How to Strengthen Constraints on Non-Newtonian Gravity from Measuring the Lateral Casimir Force

Galina L. Klimchitskaya [1,2,*] and Vladimir M. Mostepanenko [1,2,3]

[1] Central Astronomical Observatory at Pulkovo of the Russian Academy of Sciences, 196140 Saint Petersburg, Russia
[2] Peter the Great Saint Petersburg Polytechnic University, 195251 Saint Petersburg, Russia
[3] Kazan Federal University, 420008 Kazan, Russia
* Correspondence: g.klimchitskaya@gmail.com

Abstract: It has been known that in the nanometer interaction range the available experimental data do not exclude the Yukawa-type corrections to Newton's gravitational law, which exceed the Newtonian gravitational force by many orders of magnitude. The strongest constraints on the parameters of Yukawa-type interaction in this interaction range follow from the experiments on neutron scattering and from measurements of the lateral and normal Casimir forces between corrugated surfaces. In this work, we demonstrate that by optimizing the experimental configuration at the expense of the higher corrugation amplitudes and smaller periods of corrugations it is possible to considerably strengthen the currently available constraints within the wide interaction range from 4.5 to 37 nm. We show that the maximum strengthening by more than a factor of 40 is reachable for the interaction range of 19 nm.

Keywords: non-Newtonian gravity; lateral Casimir force; Yukawa-type interaction; neutron scattering; Cavendish-type experiments

check for updates

Citation: Klimchitskaya, G.L.; Mostepanenko, V.M. How to Strengthen Constraints on Non-Newtonian Gravity from Measuring the Lateral Casimir Force. *Universe* **2023**, *9*, 34. https://doi.org/10.3390/universe9010034

Academic Editors: Chitta Ranjan Das, Alexander S. Barabash and Vitalii A. Okorokov

Received: 22 December 2022
Revised: 28 December 2022
Accepted: 29 December 2022
Published: 3 Jaunary 2023

Copyright: © 2023 by the authors. Licensee MDPI, Basel, Switzerland. This article is an open access article distributed under the terms and conditions of the Creative Commons Attribution (CC BY) license (https://creativecommons.org/licenses/by/4.0/).

1. Introduction

Gravitation is the most universal interaction because it manifests itself for all macroscopic bodies as well as for elementary particles and fields. Although the gravitational force is familiar from everyday practice, the classical and quantum theories of gravitation and their correlation with the experimental data leave much to be desired. It is common knowledge that the construction of quantum gravity runs into insuperable difficulties. None of the theoretical approaches, such as string theory, or loop quantum gravity, can be considered as the comprehensive description of gravitation. Of particular surprise is the fact that even the classical Newton law of gravitation is tested with sufficient precision only at relatively large separations, whereas at submicrometer distances the corrections to Newtonian gravity, which exceed it by many orders of magnitude, are not excluded experimentally [1]. The questions arise what is the analytic form of possible corrections to Newton's law at short separations and how could they be detected or at least constrained experimentally.

The extended Standard Model, supersymmetry and supergravity predict a lot of hypothetical interactions which could coexist with Newtonian gravity at submicrometer separations (see the recent review [2] for the list of these interactions, their Lagrangian densities and forms of effective potentials). There are both spin-independent and depending on the spin of interacting particles potentials among them. It should be reminded that forces caused by the former act between any macroscopic bodies, whereas the latter are averaged to zero when integrated over the volumes of unpolarized bodies.

Particular attention has been given in the literature to the Yukawa-type interaction [1]. It is described by the spin-independent potential and acts between each pair of atoms belonging to two macrobodies. After integration over their volumes with subsequent

negative differentiation with respect to the separation distance, the Newtonian gravitational force acquires some correction.

The Yukawa-type potential is physically realized through the exchange of light scalar particles, such as, e.g., dilaton [3], predicted in extra dimensional theories where the additional dimensions are spontaneously compactified at the Planck energy scale of the order of 10^{19} GeV. Moreover, the Newtonian gravitational force in itself gains the Yukawa-type correction in the extra dimensional schemes where the spontaneous compactification occurs at a much lower energy scale of order of 1 TeV $= 10^3$ GeV [4–7]. Because of this, measuring small forces between macrobodies at short separations becomes topical as a test for predictions of fundamental physical theories.

During the last decades, different physical phenomena and associated experiments have been used for searching the non-Newtonian gravity and constraining its parameters. Although the corrections to Newton's law at short separations were not found, the constraints on the parameters of corresponding potentials, including the Yukawa one, were significantly strengthened. Thus, the stringent constraints on the Yukawa-type corrections have been obtained from the Cavendish-type [8–11] and Eötvos-type [12–14] experiments within the interaction range in excess of a few micrometers. In the interaction range of the order of 1 nm, the most strong constraints on the parameters of Yukawa-type interaction have been found from the experiments on neutron scattering on solid or gaseous targets [15–17] (see also [2] for a detailed review and [18] for a recent important result).

It is notable that in the gap from nanometers to micrometers the dominant background for searching hypothetical interactions is formed by the fluctuation-induced Casimir force, which is far in access the gravitational force within this interaction range. First constraints on the Yukawa- and power-type corrections to Newtonian gravity were obtained in [19] and [20], respectively. In succeeding years, a lot of precision experiments on measuring the Casimir force and its gradient have been performed and their results were used for obtaining stronger constraints on the Yukawa-type corrections to Newton's gravitational law [21–32] (see also [33,34] for a review).

Until recently, the strongest constraints on the Yukawa-type corrections to Newtonian gravity in the interaction range above 1 nm were obtained from the experiments on neutron scattering [16,17], measurements of the lateral [35–37] and normal [38–40] Casimir forces between the sinusoidally corrugated surfaces, effective Casimir pressure [25–28] and from the differential measurements [30], where the Casimir force was nullified. In the interaction range above 8 μm, the strongest constraints on the Yukawa-type interaction were found from the gravitational experiments [9–14].

In this paper, we consider constraints on the non-Newtonian gravity of Yukawa-type in the nanometer interaction range with account of recent strengthening achieved in the new experiment using the neutron scattering on a silicon structure [18]. According to our results, these constraints can be further strengthened by optimizing the experiment on measuring the lateral Casimir force between the sinusoidally corrugated surfaces of a sphere and a plate coated with an Au layer. It is shown that by choosing the corrugation amplitudes on a sphere and a plate equal to 33 and 90 nm, respectively, and a corrugation period of 200 nm, it becomes possible to strengthen the strongest current constraints by up to more than a factor of 40 over the interaction range from 4.5 to 37 nm. Several alternative proposals on how the constraints on the Yukawa-type interaction could be strengthened in the nanometer interaction range are discussed.

The paper is organized as follows. In Section 2, the Yukawa-type potential is considered and the strongest current constraints on its parameters are presented. Section 3 contains the derivation of prospective constraints, which could be obtained from the optimized experiment on measuring the lateral Casimir force between the sinusoidally corrugated surfaces with equal corrugation periods. The alternative proposals aimed at strengthening the current constraints in the nanometer interaction range are analyzed in Section 4. Our discussion is contained in Section 5, and we will finish with Section 6 devoted to conclusions.

2. The Yukawa-Type Potential and Current Constraints on Its Parameters in the Range from Nanometers to Micrometers

Most commonly, the Yukawa-type interaction is considered as an addition to Newtonian gravity. In this case the interaction energy between two point-like masses m_1 and m_2 spaced at a distance r takes the form [1]

$$V(r) = -\frac{Gm_1m_2}{r}(1+\alpha e^{-r/\lambda}), \tag{1}$$

where G is the Newtonian gravitational constant, α is the strength of Yukawa interaction and λ is its range.

If the Yukawa-type term in (1) originates from the exchange of light scalar particles of mass m, λ has the meaning of the Compton wavelength of this particle $\lambda = \hbar/(mc)$ where $\hbar$ is the Planck constant and c is the velocity of light. In the extra dimensional theories with the low-energy compactification scale [4–7], λ is of the order of the size of the compact manifold.

Within the interaction range up to a few nanometers, the strongest constraints on the parameters of Yukawa-type interaction α and λ follow from experiments measuring the scattered intensity of neutrons on solid, fluid or gaseous targets [41]. The measurement results are compared with the theoretical scattered intensity describing interaction of neutrons with nuclei of target atoms. The measured and theoretical scattered intensities are found in agreement in the limits of the experimental error. Then, any contribution of the Yukawa interaction to the theoretical scattered intensity must be restricted by the same error. This leads to the corresponding constraints on the Yukawa parameters α and λ.

In Figure 1, the lines labeled n_1, n_2 and n_3 show the constraints obtained from measuring the scattered intensity of neutrons on xenon and helium gases [17], atomic xenon gas [16] and on silicon [18], respectively. For these ones and all other lines, the regions of the (λ,α)-plane above each line are excluded by the results of respective experiment, whereas the regions below each line are allowed. The constraints of the lines n_1, n_2 and n_3 extend to the region $\lambda < 1$ nm. In so doing at $\lambda = 0.1$ nm the lines n_1 and n_2 intersect so that for 0.03 nm $< \lambda <$ 0.1 nm the constraints of line n_1 [17] become stronger than the constraints of line n_2 [16]. The strongest constraints in the region from 0.02 to 19 nm are, however, given by the line n_3 obtained from the recent experiment [18].

As mentioned in Section 1, the dominant background force acting between uncharged material bodies spaced at separation distances a from a few nanometers to a few micrometers is the Casimir force $F_C(a)$. The Casimir force, $F_C^{\mathrm{th}}(a)$, acting between the plane parallel structures can be calculated theoretically using the fundamental Lifshitz theory [42,43] (see also [44,45] for a formulation in modern notations). For the bodies of arbitrary shape V_1 and V_2, one should use the generalization of the Lifshitz theory valid for configurations of any geometry [46–55].

In precision measurements, the theoretical values of the Casimir force are usually found to be in agreement with the mean experimental values, $F_C^{\mathrm{expt}}(a)$, within the limits of the total experimental error $\Delta F_C(a)$, which takes into account both the random and systematic errors. One more force acting between the bodies V_1 and V_2 is obtained by integration of the interaction energy (1) over their volumes with subsequent negative differentiation with respect to separation

$$F_{\mathrm{Yu}}(a) = G\rho_1\rho_2\frac{\partial}{\partial a}\int_{V_1}d^3r_1\int_{V_2}d^3r_2\frac{1+\alpha e^{-|\boldsymbol{r}_1-\boldsymbol{r}_2|/\lambda}}{|\boldsymbol{r}_1-\boldsymbol{r}_2|}, \tag{2}$$

where ρ_1 and ρ_2 are the mass densities of the bodies.

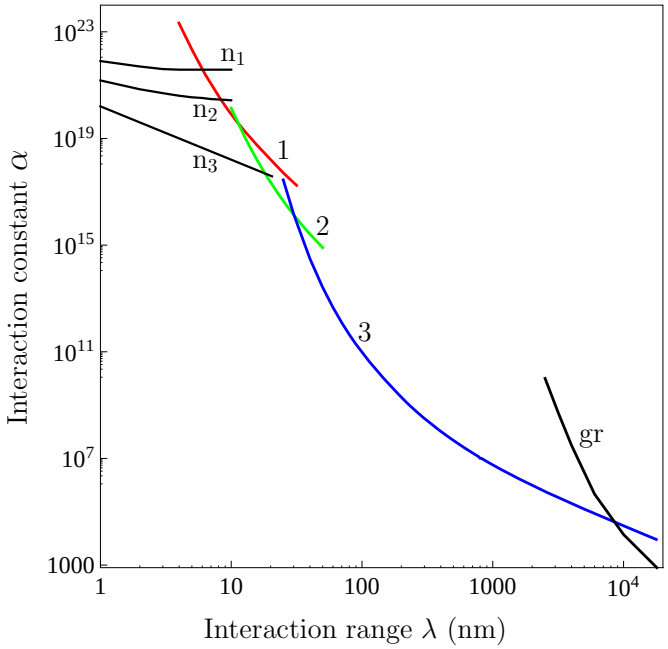

Figure 1. The constraints on the parameters of the Yukawa-type interaction obtained from the experiments on neutron scattering are shown by the lines labeled n_1 [17], n_2 [16] and n_3 [18]. The lines labeled 1, 2 and 3 show the constraints following from measuring the lateral [35–37] and normal [38–40] Casimir forces between the sinusoidally corrugated surfaces and from the differential measurements where the Casimir force was nullified [30], respectively. The line labeled gr follows from the Cavendish-type experiments. The regions of the (λ, α)-plane above each line are excluded and below each line are allowed.

Recall that in the nanometer separation range the allowable Yukawa-type corrections exceed the Newtonian gravity by many orders of magnitudes. For this reason, one can safely neglect by unity in the numerator of (2). Thus, taking into account that in precision experiments on measuring the Casimir force mentioned above the Yukawa-type interaction was not observed, the constraints on its parameters can be obtained from the inequality

$$|F_{\mathrm{Yu}}(a)| < \Delta F_C(a). \tag{3}$$

In Figure 1, the constraints obtained following this methodology are shown by the lines 1 and 2. Line 1 was found [37] from measuring the lateral Casimir force between the sinusoidally corrugated surfaces of a sphere and a plate coated with Au layers [35,36]. The corrugation amplitudes were equal to $A_1 = 85.4$ nm on the plate and $A_2 = 13.7$ nm on the sphere, whereas the corrugation periods were equal to $\Lambda_1 = \Lambda_2 = 574.7$ nm. The constraints of line 1 at different λ were obtained [37] using the measurement data at different separations: $a_1 = 121.1$ nm, where $\Delta F_C(a_1) = 11.1$ pN, $a_2 = 124.7$ nm, where $\Delta F_C(a_2) = 4.7$ pN, and $a_3 = 137.3$ nm, where $\Delta F_C(a_3) = 2.5$ pN [35,36].

The constraints of line 2 in Figure 1 were found [40] from measuring the normal Casimir force between the sinusoidally corrugated surfaces of a sphere and a plate coated with Au layers at various angles between corrugations [38,39]. In this case, the corrugation amplitudes on the plate and on the sphere were equal to $A_1 = 40.2$ nm and $A_2 = 14.6$ nm, respectively, and the corrugation period was equal to $\Lambda = 570.4$ nm. The angles between the axes of corrugations on both bodies in different measurement sets were equal to 0°, 1.2°, 1.8° and 2.4°. The constraints of line 2 were obtained at $\theta = 2.4^\circ$, $a = 127$ nm, where $\Delta F_C(a) = 0.94$ pN [38,39]. These constraints are the strongest ones in the interaction range from 19 to 30 nm.

For larger λ, the strongest constraints on the Yukawa-type interaction were found by performing the differential force measurement between an Au-coated sphere and a

structured disk consisting of Au and Si sectors coated with an Au protective layer [30]. Here, the measured quantity is the difference of forces acting on the sphere in its positions above an Au and Si sectors. Due to the presence of an overlayer, the contributions of the Casimir force to this difference are canceled, which increases the sensitivity to the presence of the Yukawa interaction. In Figure 1, the obtained constraints are the strongest ones over the interaction range from 30 to 8000 nm = 8 μm. For even larger $\lambda < 4$ mm, the strongest constraints on the parameters of Yukawa interaction follow from the Cavendish-type experiments [8–11]. The interaction ranges of micrometers and millimeters are, however, far beyond the subject of this paper.

3. Prospective Constraints from Measuring the Lateral Casimir Force between Corrugated Surfaces

In Section 2, we have considered the constraints on the Yukawa-type interaction obtained from measuring the lateral Casimir force between the sinusoidally corrugated surfaces of a sphere and a plate by means of an atomic force microscope [35,36] (see the line 1 in Figure 1). At the moment, they are not the strongest ones for any λ. In 2010, however, when these constraints were obtained [37], they were much more restrictive than all other constraints available at that time.

It is interesting to note in this connection that the experiment [35,36] was designed not for constraining the non-Newtonian gravity but for measuring the lateral Casimir force in a highly nontrivial case of sufficiently small period of corrugations. In this case, simple approximate methods for calculating the Casimir force (like the proximity force approximation) are not applicable, and it is necessary to use the generalization of the Lifshitz theory for the bodies of arbitrary shape based on the scattering theory (see Section 2). With this in mind, the lateral Casimir force was measured, compared with the exact theory, and a very good agreement was demonstrated [35,36].

As noted in [56], the constraints on the Yukawa interaction following from measurements of the lateral Casimir force can be strengthened by optimizing the experimental configuration appropriately. Below, we demonstrate that this optimization—in combination with an increased current precision of measurements—allow strengthening of previously found constraints [37] by up to a factor of 600, as compared to well known results [16] shown by the line n_2 in Figure 1, and by up to more than a factor of 40 in comparison with the most recent results shown by the line n_3 [18].

In our proposal of the optimized experiment on measuring the lateral Casimir force between the sinusoidally corrugated surfaces, we preserve the main features of the already performed experiment [35,36]. Specifically, we assume that the polystyrene sphere of density $\rho_s = 1.06 \times 10^3$ kg/m^3 with the radius $R = 97.0$ μm is coated with a layer of chromium of thickness $\Delta_{\mathrm{Cr}} = 10$ nm and density $\rho_{\mathrm{Cr}} = 7.14 \times 10^3$ kg/m^3 and by the outer gold layer of thickness $\Delta_{\mathrm{Au},s} = 50$ nm and density $\rho_{\mathrm{Au}} = 19.28 \times 10^3$ kg/m^3. The grating made of hard epoxy with density $\rho_g = 1.08 \times 10^3$ kg/m^3 on a Pyrex substrate of 3 mm thickness is used as a plate. The grating is coated with an Au layer of thickness $\Delta_{\mathrm{Au},g} = 300$ nm.

We choose only slightly larger corrugation amplitude of the grating $A_1 = 90$ nm, than it was in [35,36], and by the factor of 2.4 larger corrugation amplitude on the sphere, $A_2 = 33$ nm. For obtaining the equal corrugation periods, which is the necessary condition for initiation of the lateral Casimir force, the corrugations on the sphere should be imprinted from the grating [35,36]. To produce the stronger constraints, we choose the corrugation period of $\Lambda = 200$ nm, which is smaller than the one used in the experiment by the factor of 2.9.

There is some phase shift φ between the sinusoidal corrugations on the sphere and on the plate. Both the lateral Casimir and lateral Yukawa-type forces are obtained by the negative differentiation of the corresponding energy with respect to φ

$$F^{\mathrm{lat}}_{\mathrm{C,Yu}}(a,\varphi) = -\frac{2\pi}{\Lambda}\frac{\partial E_{\mathrm{C,Yu}}(a,\varphi)}{\partial\varphi}. \tag{4}$$

Note that for the corrugated surfaces the separation distance a is defined between the zeroth levels of corrugations.

The Yukawa energy $E_{\rm Yu}(a,\varphi)$ in the configuration of a corrugated sphere and a corrugated plate coated by the chromium and gold layers as described above is calculated by the integration of the Yukawa interaction potential over the volumes of both bodies. The result is [37]

$$E_{\rm Yu}(a,\varphi) = -4\pi^2 G\alpha\lambda^4\Psi(\lambda)e^{-a/\lambda}I_0\left(\frac{b(\varphi)}{\lambda}\right), \tag{5}$$

where $I_n(z)$ is the Bessel function of imaginary argument, the quantity $b(\varphi)$ is given by

$$b(\varphi) = \left(A_1^2 + A_2^2 - 2A_1A_2\cos\varphi\right)^{1/2}, \tag{6}$$

and the function $\Psi(\lambda)$ takes into account the layer structure of both bodies. It is defined as

$$\begin{aligned}\Psi(\lambda) = &\left[\rho_{\rm Au} - (\rho_{\rm Au}-\rho_g)e^{-\Delta_{{\rm Au},g}/\lambda}\right] \\ &\times\left[\rho_{\rm Au}\Phi(R,\lambda) - (\rho_{\rm Au}-\rho_{\rm Cr})\Phi(R-\Delta_{{\rm Au},s},\lambda)e^{-\Delta_{{\rm Au},s}/\lambda}\right. \\ &\left. - (\rho_{\rm Cr}-\rho_s)\Phi(R-\Delta_{{\rm Au},s}-\Delta_{\rm Cr},\lambda)e^{-(\Delta_{{\rm Au},s}+\Delta_{\rm Cr})/\lambda}\right],\end{aligned} \tag{7}$$

where

$$\Phi(x,\lambda) \equiv x - \lambda + (x+\lambda)e^{-2x/\lambda}. \tag{8}$$

Substituting (5) in (4), one obtains the analytic expression for the lateral Yukawa force in the experimental configuration used to measure the lateral Casimir force

$$F_{\rm Yu}^{\rm lat}(a,\varphi) = 8\pi^3 G\alpha\lambda^3\Psi(\lambda)e^{-a/\lambda}\frac{A_1A_2}{b(\varphi)\Lambda}I_1\left(\frac{b(\varphi)}{\lambda}\right)\sin\varphi. \tag{9}$$

The constraints on the parameters of Yukawa interaction are obtained from the inequality

$$|F_{\rm Yu}^{\rm lat}(a,\varphi)| < \Delta F_C^{\rm lat}(a), \tag{10}$$

where, in this case, $\Delta F_C^{\rm lat}(a)$ is the total experimental error in measuring the lateral Casimir force, which is the measure of agreement between the obtained data and the exact theory.

The values of $\Delta F_C^{\rm lat}(a)$ to be used for obtaining prospective constraints on the Yukawa-type corrections to Newtonian gravity deserve special attention. Taking into account larger values of the corrugation amplitudes chosen for the prospective experiment, the minimum separation distance in this case can be taken as $\tilde{a}_1 = 125$ nm (this is approximately equal to the second shortest separation a_2 in the experiment [35,36]). The third shortest separation in [35,36] was $a_3 = 137.3$ nm. This value is used as the second shortest separation $\tilde{a}_2$ in the prospective experiment. Taking into account that in a time passed after the experiment [35,36] was performed the measure of agreement between measurements of the Casimir force by means of an atomic force microscope and theory was improved by an order of magnitude [57], we put $\Delta F_C^{\rm lat}(\tilde{a}_1) = 1.11$ pN and $\Delta F_C^{\rm lat}(\tilde{a}_2) = 0.47$ pN (see Section 2). Note that an improvement in agreement between the measurement data and theory was achieved by a significant decrease in the residual potential difference between a sphere and a plate and the use of the cantilever of an atomic force microscope with by an order of magnitude smaller spring constant. The latter resulted in a factor of 10 larger calibration constant and corresponding decrease of the systematic error in force measurements [57,58].

As a result, the prospective constraints on the Yukawa-type interaction which can be obtained from the optimized experiment on measuring the lateral Casimir force, are found from (9) and (10) with $a = \tilde{a}_1$ and $\tilde{a}_2$. These constraints are shown by the dashed line in Figure 2. For comparison purposes, in Figure 2 we reproduce from Figure 1 the lines labeled $\rm n_1$, $\rm n_2$ and $\rm n_3$ found from the experiments on neutron scattering [16–18], and

the lines labeled 1, 2 and 3 obtained from the already performed measurement of the lateral [35–37] and normal [38–40] Casimir forces between the sinusoidally corrugated surfaces and from the differential measurement where the Casimir force was nullified [30].

As seen in Figure 2, the constraints shown by the dashed line are the strongest ones in the interaction range from 4.5 nm to 37 nm. The greatest strengthening by the factor of 41 holds at $\lambda = 19$ nm. If, to exclude from comparison, the recent result obtained from the neutron scattering on a silicon target (line n_3) [18] and compare the dashed line with the line n_2 [16], the greatest strengthening would be up to a factor of 600.

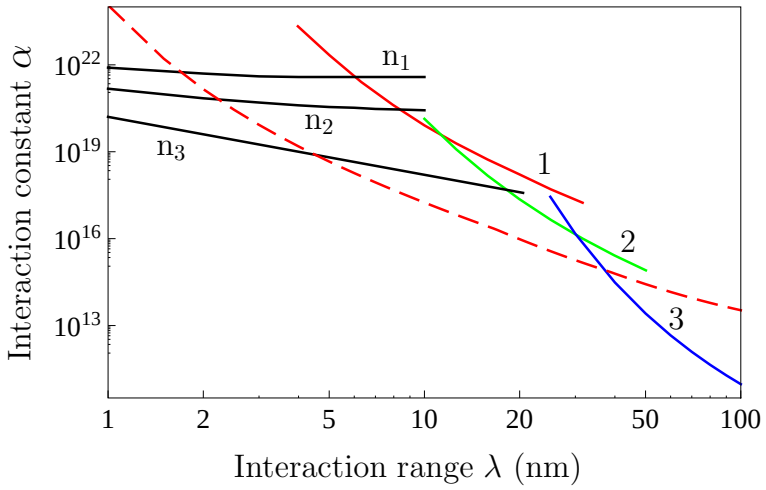

Figure 2. The constraints on the parameters of the Yukawa-type interaction, which can be obtained from the optimized experiment on measuring the lateral Casimir forces between the sinusoidally corrugated surfaces are shown by the dashed line. The lines labeled n_1 [17], n_2 [16] and n_3 [18] show the constraints following from the experiments on neutron scattering. The lines labeled 1, 2 and 3 show the constraints following from measurements of the lateral [35–37] and normal [38–40] Casimir forces between corrugated surfaces and from the differential measurements [30]. The regions of the (λ, α)-plane above each line are excluded and below each line are allowed.

Thus, experiments measuring the Casimir force have potentialities for strengthening the constraints on the Yukawa-type corrections to Newtonian gravity and can compete on this point with the experiments on neutron scattering. In the next section, we consider some more suggestions recently proposed in the literature, which are directed to further strengthening of the already obtained constraints.

4. Several Alternative Proposals

As discussed in previous sections, the experiments on neutron scattering are actively used for constraining the Yukawa-type corrections to Newton's gravitational law. It was also suggested [59] to constrain both the axion-like particles and the parameters of Yukawa-type potentials by means of interferometric measurements of neutron beams. In this case, the source beam is split into two parts, which propagate through differently oriented magnetic fields and then interfere. Note that it was also suggested [60] to use the neutron interferometry in extra dimensional physics with the low-energy compactification scale for constraining the Yukawa-type corrections to Newtonian gravity (see Section 1). The compactification radius of large extra dimensions, which is directly connected with the parameter λ of the Yukawa-type potential, was recently constrained using the datasets of several neutrino experiments [61].

The spectroscopic measurements in weakly bound molecules can also be used for constraining the Yukawa-type interaction between atoms. Thus, it was shown [62] that the measurement data of the new spectroscopic technique of photoassociation of Yb_2 molecules constrain the non-Newtonian gravity in much the same manner as the experiments on

neutron scattering. It was argued [62] that in combination with the optical molecular clocks the spectroscopic measurements in weakly bound molecules could result in up to two orders of magnitude stronger constraints on non-Newtonian gravity than the experiments on neutron scattering. Molecular spectroscopy was also used for constraining different kinds of potentials predicted in various extensions of the Standard Model [63].

According to the proposal of [64], the spectroscopic measurements of ionic transitions between the Rydberg states of electronic and muonic ions lead to prospective constraints on non-Newtonian gravity in the nanometer interaction range, which are stronger than those obtained from neutron scattering and measuring the Casimir force. A rather wide interaction range of the constraints, which can be obtained by using the muonic ions (from 10^{-4} to 10 nm), is explained in [64] by the very high precision in measuring the Rydberg transitions in the optical frequency region.

There are also several more suggestions in the literature devoted to obtaining stronger constraints on non-Newtonian gravity at short separations. Thus, the optical setup proposed in [65] consists of a mirror and a source mass. A silica nanosphere is trapped near the surface of a source mass. Similar to experiments on measuring the Casimir force in the dynamic regime [26–28], the difference in the actual resonance frequency of this nanosphere results from the total force gradient acting on it. By comparing the measurement results with calculations in this configuration, it is possible to strengthen the current constraints on the parameters of Yukawa-type interaction. In essence, this suggestion is similar in spirit to the experiment on measuring the thermal Casimir–Polder force between a cloud of ^{87}Rb atoms belonging to the Bose–Einstein condensate and a SiO_2 plate [66]. In this experiment, the atomic cloud was resonantly driven into a dipole oscillation by a magnetic field, and the measured quantity was the frequency shift caused by the Casimir–Polder force. The constraints on the Yukawa-type interaction following from the measurement data of [66] were obtained in [37]. According to the results of [65], the use of a nanosphere allows obtaining up to two orders of magnitude stronger constraints over the interaction range from 100 nm to 10 μm. This is, however, beyond the nanometer interaction range considered in Section 3.

Recently, the new Cavendish-type experiment was performed [11,67], which is especially optimized in order to increase the possible impact of the Yukawa-type interaction. This was achieved by substantially increasing the areas of both the source and test masses. As a result, up to an order of magnitude strengthening of the constraints on the constant α of Yukawa-type interaction was reached in the range from 40 to 800 μm, which is not shown in Figure 1.

One more suggestion for searching the non-Newtonian gravity is to perform the microscope Eötvos-type experiment, which should test the weak equivalence principle [68]. For this purpose, it is planned to compare the low-frequency dynamics of the free-falling test masses of cylindrical form controlled by electrostatic forces. The expected constraints should span the interaction range from 100 μm to 1 m far away from the subject of our concern.

There are also proposals of new experiments on measuring the Casimir–Polder and Casimir forces. Thus, it was shown [69] that measurements of the Casimir–Polder force between a Rb atom and a movable Si plate shielded by the Au film can be used for obtaining up to two orders of magnitude stronger constraints on the Yukawa-type corrections to Newtonian gravity in the interaction range from a fraction of micrometer to 10 μm. Within the same interaction range, the current constraints can be strengthened by an order of magnitude from the experiment measuring the Casimir pressure and its gradient between two parallel plates at micrometer separations [70,71].

In the end of this section, we mention the proposal for testing the corrections to Newtonian gravity in the submillimeter and submicrometer ranges by using the optical system with extremely high temporal precision [72]. It remains unknown, however, how strong constraints could be obtained by using this experimental approach.

5. Discussion

In the foregoing, we have considered the corrections to Newtonian gravity in the nanometer interaction range and different possibilities for their strengthening. During the last few years, the strongest constraints on non-Newtonian gravity in this interaction range were obtained from the experiments on neutron scattering and from measurements of the lateral and normal Casimir forces between the sinusoidally corrugated surfaces of a sphere and a plate. Somewhat weaker constraints were found from the experiments on measuring the Casimir force between a microsphere coated with an Au layer and a silicon carbide plate spaced at the minimum separation of 10 nm [73–75] and the phase shifts caused by the Casimir–Polder interaction between Li atoms and a silicon nitride grating [76].

It should be noted that the recent experiment on neutron scattering [18] (see the line n_3 in Figures 1 and 2) has extended the interaction range, where the neutron experiments lead to the strongest constraints on the Yukawa-type corrections to Newtonian gravity, up to 19 nm. However, as shown in this paper, measurements of the lateral Casimir force have a good chance to become the strongest ones in the interaction range from 4.5 to 37 nm. This means that some kind of competition between the experiments on neutron scattering and measurements of the Casimir force in obtaining constraints at nanometers is being continued. One can guess that the spectroscopic measurements [77] will also take part in this competition.

The derivation of constraints on non-Newtonian gravity from measurements of the Casimir force is essentially based on the comparison between experiment and theory. It has been known, however, that this comparison is complicated by the problem of relaxation properties of conduction electrons. This problem lies in the fact that theoretical predictions of the Lifshitz theory are in good agreement with the measurement data only if the relaxation properties of conduction electrons are omitted in computations. If, however, the relaxation properties are taken into account, the theoretical predictions are excluded by the data [25–31,44,45,57,78]. The necessity of considering the real material properties, specific geometry of the interacting bodies and the effect of thermal fluctuations in calculations of the Casimir force was underlined in [79–81]. According to [80,81], if the objective of some particular experiment is to test the model of material properties, that experiment should not be used for constraining the hypothetical interactions. During the past ten years, however, many problems in computation of the Casimir force mentioned in [79–81] found a solution. Thus, the decisive differential measurement [82], where the predictions of the Lifshitz theory with omitted and included relaxation properties of conduction electrons differ by up to the factor of 1000, conclusively established that for reaching an agreement with the experimental data the computational approach should omit the relaxation properties of conduction electrons. An active search for the theoretical justification of this approach is in progress [83,84]. It is pertinent to note, however, that both theoretical approaches lead to almost equal results for the lateral and normal Casimir forces between the sinusoidally corrugated surfaces at short separations used for obtaining the constraints on non-Newtonian gravity in the nanometer interaction range (see lines 1 and 2 in Figures 1 and 2). In a similar way, the mentioned distinction between the theoretical approaches makes no impact on the results of the Casimir-less experiment [30], where the contribution of the Casimir force is canceled (see the line 3 in Figures 1 and 2).

In spite of a notable advance, which has been made in obtaining stronger constraints on the Yukawa-type corrections to Newtonian gravity in the nanometer interaction range, much remains to be done. The point is that the corrections exceeding the Newton force by up to 19 orders of magnitude are still not ruled out by the measurement data in the range of a few nanometers. This is not an entirely academic problem related to such fundamental unresolved issues as, e.g., the nature of dark matter [2,85]. As an example, the Yukawa-type corrections to Newton's law make an impact on the properties of strange quark stars. Specifically, it is shown that observations of some astrophysical events using the MIT bag model cannot be explained if the effects of non-Newtonian gravity are disregarded [86]. In this connection, an investigation of different kinds of additional forces predicted by the

fundamental physics (they are often referred to by the generic name *the fifth force* and the experimental limits imposed on their parameters deserve further attention [87].

6. Conclusions

To conclude, the strongest current constraints on the Yukawa-type corrections to Newton's gravitational law in the nanometer interaction range follow from the recent experiment on neutron scattering (see line n_3 in Figure 2), from measuring the normal Casimir force between the sinusoidally corrugated surfaces (see line 2 in Figure 2), and from the differential measurement where the Casimir force is nullified (see line 3 in the same figure).

According to our results, these constraints can be strengthened by up to a factor of 41 based on the experiment measuring the lateral Casimir force between the sinusoidally corrugated surfaces of a sphere and a plate. We propose this experiment as a modification of the already performed measurement of the lateral Casimir force optimized in order to obtain the strongest constraints achievable in this configuration. Our calculations show that the strengthening can be obtained in the interaction range from 4.5 to 37 nm. This would narrow the interaction region, where the strongest constraints follow from the experiments on neutron scattering, and exclude measurements of the normal Casimir force between the sinusoidally corrugated surfaces from the list of experiments leading to the strongest constraints on non-Newtonian gravity of Yukawa-type in the nanometer interaction range.

In the near future one could expect new results in this rapidly progressing field obtained from the repetitions and modifications of the experiments mentioned above, as well as from the alternative experimental tests based on some other physical phenomena.

Author Contributions: Conceptualization, G.L.K. and V.M.M.; investigation, G.L.K. and V.M.M.; writing—original draft, V.M.M.; writing—review and editing, G.L.K. and V.M.M. All authors have read and agreed to the published version of the manuscript.

Funding: The work of V.M.M. was supported by the Kazan Federal University Strategic Academic Leadership Program.

Institutional Review Board Statement: Not applicable.

Informed Consent Statement: Not applicable.

Data Availability Statement: Not applicable.

Acknowledgments: The authors are grateful to U. Mohideen who suggested to measure the lateral Casimir force and performed the experiment [35,36].

Conflicts of Interest: The authors declare no conflict of interest.

References

1. Fischbach, E.; Talmadge, C.L. *The Search for Non-Newtonian Gravity*; Springer: New York, NY, USA, 1999.
2. Sponar, S.; Sedmik, R.I.P.; Pitschmann, M.; Abele, H.; Hasegawa, Y. Tests of fundamental quantum mechanics and dark interactions with low-energy neutrons. *Nat. Rev. Phys.* **2021**, *3*, 309–327. [CrossRef]
3. Fujii, Y. The theoretical background of the fifth force. *Int. J. Mod. Phys. A* **1991**, *6*, 3505–3557. [CrossRef]
4. Antoniadis, I.; Arkani-Hamed, N.; Dimopoulos, S.; Dvali, G. New dimensions at a millimeter to a fermi and superstrings at a TeV. *Phys. Lett. B* **1998**, *436*, 257–263. [CrossRef]
5. Arkani-Hamed, N.; Dimopoulos, S.; Dvali, G. Phenomenology, astrophysics, and cosmology of theories with millimeter dimensions and TeV scale quantum gravity. *Phys. Rev. D* **1999**, *59*, 086004. [CrossRef]
6. Floratos, E.G.; Leontaris, G.K. Low scale unification, Newton's law and extra dimensions. *Phys. Lett. B* **1999**, *465*, 95–100. [CrossRef]
7. Kehagias, A.; Sfetsos, K. Deviations from $1/r^2$ Newton law due to extra dimensions. *Phys. Lett. B* **2000**, *472*, 39–44. [CrossRef]
8. Smullin, S.J.; Geraci, A.A.; Weld, D.M.; Chiaverini, J.; Holmes, S.; Kapitulnik, A. Constraints on Yukawa-type deviations from Newtonian gravity at 20 microns. *Phys. Rev. D* **2005**, *72*, 122001. [CrossRef]
9. Adelberger, E.G.; Heckel, B.R.; Hoedl, S.; Hoyle, C.D.; Kapner, D.J.; Upadhye, A. Particle-Physics Implications of a Recent Test of the Gravitational Inverse-Square Law. *Phys. Rev. Lett.* **2007**, *98*, 131104. [CrossRef]
10. Kapner, D.J.; Cook, T.S.; Adelberger, E.G.; Gundlach, J.H.; Heckel, B.R.; Hoyle, C.D.; Swanson, H.E. Tests of the Gravitational Inverse-Square Law below the Dark-Energy Length Scale. *Phys. Rev. Lett.* **2007**, *98*, 021101. [CrossRef]

11. Tan, W.-H.; Du, A.-B.; Dong, W.-C.; Yang, S.-Q.; Shao, C.-G.; Guan, S.-G.; Wang, Q.-L.; Zhan, B.-F.; Luo, P.-S.; Tu, L.-C.; et al. Improvement for Testing the Gravitational Inverse-Square Law at the Submillimeter Range. *Phys. Rev. Lett.* **2020**, *124*, 051301. [CrossRef]
12. Gundlach, J.H.; Smith, G.L.; Adelberger, E.G.; Heckel, B.R.; Swanson, H.E. Short-Range Test of the Equivalence Principle. *Phys. Rev. Lett.* **1997**, *78*, 2523–2526. [CrossRef]
13. Smith, G.L.; Hoyle, C.D.; Gundlach, J.H.; Adelberger, E.G.; Heckel, B.R.; Swanson, H.E. Short-range tests of the equivalence principle. *Phys. Rev. D* **2000**, *61*, 022001. [CrossRef]
14. Schlamminger, S.; Choi, K.-J.; Wagner, T.A.; Gundlach, J.H.; Adelberger, E.G. Test of the Equivalence Principle Using a Rotating Torsion Balance. *Phys. Rev. Lett.* **2008**, *100*, 041101. [CrossRef] [PubMed]
15. Nesvizhevsky, V.V.; Pignol, G.; Protasov, K.V. Neutron scattering and extra short range interactions. *Phys. Rev. D* **2008**, *77*, 034020. [CrossRef]
16. Kamiya, Y.; Itagami, K.; Tani, M.; Kim, G.N.; Komamiya, S. Constraints on New Gravitylike Forces in the Nanometer Range. *Phys. Rev. Lett.* **2015**, *114*, 161101. [CrossRef]
17. Haddock, C.C.; Oi, N.; Hirota, K.; Ino, T.; Kitaguchi, M.; Matsumoto, S.; Mishima, K.; Shima, T.; Shimizu, H.M.; Snow, W.M.; et al. Search for deviations from the inverse square law of gravity at nm range using a pulsed neutron beam. *Phys. Rev. D* **2018**, *97*, 062002. [CrossRef]
18. Heacock, B.; Fujiie, T.; Haun, R.W.; Henins, A.; Hirota, K.; Hosobata, T.; Huber, M.G.; Kitaguchi, M.; Pushin, D.A.; Shimizu, H.; et al. Pendellösung interferometry probes the neutron charge radius, lattice dynamics, and fifth forces. *Science* **2021**, *373*, 1239–1243. [CrossRef]
19. Kuzmin, V.A.; Tkachev, I.I.; Shaposhnikov, M.E. Restrictions imposed on light scalar particles by measurements of van der Waals forces. *Pis'ma V Zh. Eksp. Teor. Fiz.* **1982**, *36*, 49–52; Translated: *JETP Lett.* **1982**, *36*, 59–62.
20. Mostepanenko, V.M.; Sokolov, I.Y. The Casimir effect leads to new restrictions on long-range force constants. *Phys. Lett. A* **1987**, *125*, 405–408. [CrossRef]
21. Mohideen, U.; Roy, A. Precision Measurement of the Casimir Force from 0.1 to 0.9 μm. *Phys. Rev. Lett.* **1998**, *81*, 4549–4552. [CrossRef]
22. Bordag, M.; Geyer, B.; Klimchitskaya, G.L.; Mostepanenko, V.M. Stronger constraints for nanometer scale Yukawa-type hypothetical interactions from the new measurement of the Casimir force. *Phys. Rev. D* **1999**, *60*, 055004. [CrossRef]
23. Ederth, T. Template-stripped gold surfaces with 0.4-nm rms roughness suitable for force measurements: Application to the Casimir force in the 20–100-nm range. *Phys. Rev. A* **2000**, *62*, 062104. [CrossRef]
24. Mostepanenko, V.M.; Novello, M. Constraints on non-Newtonian gravity from the Casimir force measurements between two crossed cylinders. *Phys. Rev. D* **2001**, *63*, 115003. [CrossRef]
25. Decca, R.S.; Fischbach, E.; Klimchitskaya, G.L.; Krause, D.E.; López, D.; Mostepanenko, V.M. Improved tests of extra-dimensional physics and thermal quantum field theory from new Casimir force measurements. *Phys. Rev. D* **2003**, *68*, 116003. [CrossRef]
26. Decca, R.S.; López, D.; Fischbach, E.; Klimchitskaya, G.L.; Krause, D.E.; Mostepanenko, V.M. Precise comparison of theory and new experiment for the Casimir force leads to stronger constraints on thermal quantum effects and long-range interactions. *Ann. Phys. (N.Y.)* **2005**, *318*, 37–80. [CrossRef]
27. Decca, R.S.; López, D.; Fischbach, E.; Klimchitskaya, G.L.; Krause, D.E.; Mostepanenko, V.M. Tests of new physics from precise measurements of the Casimir pressure between two gold-coated plates. *Phys. Rev. D* **2007**, *75*, 077101. [CrossRef]
28. Decca, R.S.; López, D.; Fischbach, E.; Klimchitskaya, G.L.; Krause, D.E.; Mostepanenko, V.M. Novel constraints on light elementary particles and extra-dimensional physics from the Casimir effect. *Eur. Phys. J. C* **2007**, *51*, 963–975. [CrossRef]
29. Decca, R.S.; López, D.; Chan, H.B.; Fischbach, E.; Krause, D.E.; Jamell, C.R. Constraining New Forces in the Casimir Regime Using the Isoelectronic Technique. *Phys. Rev. Lett.* **2005**, *94*, 240401. [CrossRef]
30. Chen, Y.J.; Tham, W.K.; Krause, D.E.; López, D.; Fischbach, E.; Decca, R.S. Stronger Limits on Hypothetical Yukawa Interactions in the 30–8000 Nm Range. *Phys. Rev. Lett.* **2016**, *116*, 221102. [CrossRef]
31. Bimonte, G.; Spreng, B.; Maia Neto, P.A.; Ingold, G.-L.; Klimchitskaya, G.L.; Mostepanenko, V.M.; Decca, R.S. Measurement of the Casimir Force between 0.2 and 8 μm: Experimental Procedures and Comparison with Theory. *Universe* **2021**, *7*, 93. [CrossRef]
32. Klimchitskaya, G.L.; Mostepanenko, V.M. Dark Matter Axions, Non-Newtonian Gravity and Constraints on Them from Recent Measurements of the Casimir Force in the Micrometer Separation Range. *Universe* **2021**, *7*, 343. [CrossRef]
33. Mostepanenko, V.M.; Klimchitskaya, G.L. The State of the Art in Constraining Axion-to-Nucleon Coupling and Non-Newtonian Gravity from Laboratory Experiments. *Universe* **2020**, *6*, 147. [CrossRef]
34. Klimchitskaya, G.L. Constraints on Theoretical Predictions beyond the Standard Model from the Casimir Effect and Some Other Tabletop Physics. *Universe* **2021**, *7*, 47. [CrossRef]
35. Chiu, H.C.; Klimchitskaya, G.L.; Marachevsky, V.N.; Mostepanenko, V.M.; Mohideen, U. Demonstration of the asymmetric lateral Casimir force between corrugated surfaces in the nonadditive regime. *Phys. Rev. B* **2009**, *80*, 121402(R). [CrossRef]
36. Chiu, H.C.; Klimchitskaya, G.L.; Marachevsky, V.N.; Mostepanenko, V.M.; Mohideen, U. Lateral Casimir force between sinusoidally corrugated surfaces: Asymmetric profiles, deviations from the proximity force approximation, and comparison with exact theory. *Phys. Rev. B* **2010**, *81*, 115417. [CrossRef]
37. Bezerra, V.B.; Klimchitskaya, G.L.; Mostepanenko, V.M.; Romero, C. Advance and prospects in constraining the Yukawa-type corrections to Newtonian gravity from the Casimir effect. *Phys. Rev. D* **2010**, *81*, 055003. [CrossRef]

38. Banishev, A.A.; Wagner, J.; Emig, T.; Zandi, R.; Mohideen, U. Demonstration of Angle-Dependent Casimir Force between Corrugations. *Phys. Rev. Lett.* **2013**, *110*, 250403. [CrossRef]
39. Banishev, A.A.; Wagner, J.; Emig, T.; Zandi, R.; Mohideen, U. Experimental and theoretical investigation of the angular dependence of the Casimir force between sinusoidally corrugated surfaces. *Phys. Rev. B* **2014**, *89*, 235436. [CrossRef]
40. Klimchitskaya, G.L.; Mohideen, U.; Mostepanenko, V.M. Constraints on corrections to Newtonian gravity from two recent measurements of the Casimir interaction between metallic surfaces. *Phys. Rev. D* **2013**, *87*, 125031. [CrossRef]
41. Willis, B.T.M.; Cartile, C.J. *Experimental Neutron Scattering*; Oxford University Press: Oxford, UK, 2009.
42. Lifshitz, E.M. The theory of molecular attractive forces between solids. *Zh. Eksp. Teor. Fiz.* **1955**, *29*, 94–110; Translated: *Sov. Phys. JETP* **1956**, *2*, 73–83.
43. Dzyaloshinskii, I.E.; Lifshitz, E.M.; Pitaevskii, L.P. The general theory of van der Waals forces. *Usp. Fiz. Nauk* **1961**, *73*, 381–422; Translated: *Adv. Phys.* **1961**, *10*, 165–209. [CrossRef]
44. Bordag, M.; Klimchitskaya, G.L.; Mohideen, U.; Mostepanenko, V.M. *Advances in the Casimir Effect*; Oxford University Press: Oxford, UK, 2015.
45. Klimchitskaya, G.L.; Mohideen, U.; Mostepanenko, V.M. The Casimir force between real materials: Experiment and theory. *Rev. Mod. Phys.* **2009**, *81*, 1827–1885. [CrossRef]
46. Emig, T.; Jaffe, R.L.; Kardar, M.; Scardicchio, A. Casimir Interaction between a Plate and a Cylinder. *Phys. Rev. Lett.* **2006**, *96*, 080403. [CrossRef] [PubMed]
47. Bordag, M. Casimir effect for a sphere and a cylinder in front of a plane and corrections to the proximity force theorem. *Phys. Rev. D 2006*, *73*, 125018. [CrossRef]
48. Emig, T.; Graham, N.; Jaffe, R.L.; Kardar, M. Casimir Forces Between Arbitrary Compact Objects. *Phys. Rev. Lett.* **2007**, *99*, 170403. [CrossRef]
49. Kenneth, O.; Klich, I. Casimir forces in a T-operator approach. *Phys. Rev. B* **2008**, *78*, 014103. [CrossRef]
50. Reynaud, S.; Maia Neto, P.A.; Lambrecht, A. Casimir energy and geometry: Beyond the proximity force approximation. *J. Phys. A Math. Theor.* **2008**, *41*, 164004. [CrossRef]
51. Rahi, S.J.; Emig, T.; Graham, N.; Jaffe, R.L.; Kardar, M. Scattering theory approach to electromagnetic Casimir forces. *Phys. Rev. D* **2009**, *80*, 085021. [CrossRef]
52. Canaguier-Durand, A.; Maia Neto, P.A.; Cavero-Pelaez, I.; Lambrecht, A.; Reynaud, S. Casimir Interaction between Plane and Spherical Metallic Surfaces. *Phys. Rev. Lett.* **2009**, *102*, 230404. [CrossRef]
53. Fosco, C.D.; Lombardo, F.C.; Mazzitelli, F.D. Proximity force approximation for the Casimir energy as a derivative expansion. *Phys. Rev. D* **2011**, *84*, 105031. [CrossRef]
54. Bimonte, G.; Emig, T.; Jaffe, R.L.; Kardar, M. Casimir forces beyond the proximity force approximation. *Europhys. Lett.* **2012**, *97*, 50001. [CrossRef]
55. Spreng, B.; Hartmann, M.; Henning, V.; Maia Neto, P.A.; Ingold, G.-L. Proximity force approximation and specular reflection: Application of the WKB limit of Mie scattering to the Casimir effect. *Phys. Rev. A* **2018**, *97*, 062504. [CrossRef]
56. Klimchitskaya, G.L. Recent breakthrough and outlook in constraining the non-Newtonian gravity and axion-like particles from Casimir physics. *Eur. Phys. J. C* **2017**, *77*, 315. [CrossRef]
57. Liu, M.; Xu, J.; Klimchitskaya, G.L.; Mostepanenko, V.M.; Mohideen, U. Examining the Casimir puzzle with an upgraded AFM-based technique and advanced surface cleaning. *Phys. Rev. B* **2019**, *100*, 081406(R). [CrossRef]
58. Liu, M.; Schafer, R.; Xu, J.; Mohideen, U. Elimination of electrostatic forces in precision Casimir force measurements using UV and Argon ion radiation. *Mod. Phys. Lett.* **2020**, *35*, 2040001. [CrossRef]
59. Capolupo, A.; Giampaolo, S.M.; Quaranta, A. Neutron interferometry, fifth force and axion like particles. *Eur. Phys. J. C* **2021**, *81*, 1116. [CrossRef]
60. Rocha, J.M.; Dahia, F. Neutron interferometry and tests of short-range modifications of gravity. *Phys. Rev. D* **2021**, *103*, 124014. [CrossRef]
61. Forero, D.V.; Giunti, C.; Ternes, C.A.; Tyagi, O. Large extra dimensions and neutrino experiments. *Phys. Rev. D* **2022**, *106*, 035027. [CrossRef]
62. Borkowski, M.; Buchachenko, A.A.; Ciuryło, R.; Julienne, P.S.; Yamada, H.; Kikuchi, Y.; Takasu, Y.; Takahashi, Y. Weakly bound molecules as sensors of new gravitylike forces. *Sci. Rep.* **2019**, *9*, 14807. [CrossRef]
63. Hollik, W.G.; Linster, M.; Tabet, T. A study of New Physics searches with tritium and similar molecules. *Eur. Phys. J. C* **2020**, *80*, 661. [CrossRef]
64. Lemos, A.S. Submillimeter constraints for non-Newtonian gravity from spectroscopy. *Europhys. Lett.* **2021**, *135*, 11001. [CrossRef]
65. Chen, L.; Liu, J.; Zhu, K.-D. Constraining the axion-nucleon coupling and non-Newtonian gravity with a levitated optomechanical device. *Phys. Rev. D* **2022**, *106*, 095007. [CrossRef]
66. Obrecht, J.M.; Wild, R.J.; Antezza, M.; Pitaevskii, L.P.; Stringari, S.; Cornell, E.A. Measurement of the temperature dependence of the Casimir-Polder force. *Phys. Rev. Lett.* **2007**, *98*, 063201. [CrossRef] [PubMed]
67. Du, A.-B.; Tan, W.-H.; Dong, W.-C.; Huang, H.; Zhu, L.; Tan, Y.-J.; Shao, C.-G.; Yang, S.-Q.; Luo, J. A new design for testing the gravitational inverse-square law at the sub-millimeter range with a 32-fold symmetric attractor. *Class. Quantum Grav.* **2022**, *39*, 105008. [CrossRef]

68. Bergé, J.; Pernot-Borràs, M.; Uzan, J.-P.; Brax, P.; Chhun, R.; Métris, G.; Rodrigues, M.; Touboul, P. MICROSCOPE's constraint on a short-range fifth force. *Class. Quantum Grav.* **2022**, *39*, 204010. [CrossRef]
69. Bennett, R.; O'Dell, D.H.J. Revealing short-range non-Newtonian gravity through Casimir-Polder shielding. *New J. Phys.* **2019**, *21*, 033032. [CrossRef]
70. Klimchitskaya, G.L.; Mostepanenko, V.M.; Sedmik, R.I.P.; Abele, H. Prospects for Searching Thermal Effects, Non-Newtonian Gravity and Axion-Like Particles: CANNEX Test of the Quantum Vacuum. *Symmetry* **2019**, *11*, 407. [CrossRef]
71. Sedmik, R.I.P. Casimir and non-Newtonian force experiment (CANNEX): Review, status, and outlook. *Int. J. Mod. Phys. A* **2020**, *35*, 2040008. [CrossRef]
72. Faizal, M.; Patel, H. Probing Short Distance Gravity using Temporal Lensing. *Int. J. Mod. Phys. A* **2021**, *36*, 2150115. [CrossRef]
73. Klimchitskaya, G.L.; Kuusk, P.; Mostepanenko, V.M. Constraints on non-Newtonian gravity and axionlike particles from measuring the Casimir force in nanometer separation range. *Phys. Rev. D* **2020**, *101*, 056013. [CrossRef]
74. Sedighi, M.; Svetovoy, V.B.; Broer, W.H.; Palasantzas, G. Casimir forces from conductive silicon carbide surfaces. *Phys. Rev. B* **2014**, *89*, 195440. [CrossRef]
75. Sedighi, M.; Svetovoy, V.B.; Palasantzas, G. Casimir force measurements from silicon carbide surfaces. *Phys. Rev. B* **2016**, *93*, 085434. [CrossRef]
76. Lepoutre, S.; Jelassi, H.; Lonij, V.P.A.; Trénec, G.; Büchner, M.; Cronin, A.D.; Vigué, J. Dispersive atom interferometry phase shifts due to atom-surface interactions. *Europhys. Lett.* **2009**, *88*, 20002. [CrossRef]
77. Safronova, M.S.; Budker, D.; DeMille, D.; Jackson Kimball, D.F.; Derevianko, A.; Clark, C.W. Search for new physics with atoms and molecules. *Rev. Mod. Phys.* **2018**, *90*, 025008. [CrossRef]
78. Mostepanenko, V.M. Casimir Puzzle and Conundrum: Discovery and Search for Resolution. *Universe* **2021**, *7*, 84. [CrossRef]
79. Antoniadis, I.; Baessler, S.; Büchner, M.; Fedorov, V.V.; Hoedl, S.; Lambrecht, A.; Nesvizhevsky, V.V.; Pignol, G.; Protasov, K.V.; Reynaud, S.; et al. Short-range fundamental forces. *Compt. Rend.* **2011**, *12*, 755–778. [CrossRef]
80. Lambrecht, A.; Reynaud, S. Casimir and short-range gravity tests. In *Gravitational Waves and Experimental Gravity*; Augé, E., Dumarchez, J., Vân, J.T.T., Eds.; Thê Gioi Publishers: Hanoi, Vietnam, 2011; pp. 199–206.
81. Lambrecht, A.; Canaguier-Durand, A.; Guérout, R.; Reynaud, S. Casimir effect in the scattering approach: Correlations between material properties, temperature and geometry. In *Casimir Physics*; Dalvit, D.A.R., Milonni, P.W., Roberts, D.C., Rosa, F.S.S., Eds.; Springer: Heidelberg, Germany, 2011; pp. 97–127.
82. Bimonte, G.; López, D.; Decca, R.S. Isoelectronic determination of the thermal Casimir force. *Phys. Rev. B* **2016**, *93*, 184434. [CrossRef]
83. Klimchitskaya, G.L.; Mostepanenko, V.M.; Svetovoy, V.B. Probing the response of metals to low-frequency s-polarized evanescent fields. *Europhys. Lett.* **2022**, *139*, 66001. [CrossRef]
84. Klimchitskaya, G.L.; Mostepanenko, V.M.; Svetovoy, V.B. *Experimentum crucis* for electromagnetic response of metals to evanescent waves and the Casimir puzzle. *Universe* **2022**, *8*, 574. [CrossRef]
85. Bertone, G.; Hooper, D. History of Dark Matter. *Rev. Mod. Phys.* **2018**, *90*, 045002. [CrossRef]
86. Yang, S.-H.; Pi, C.-M.; Zheng, X.-P.; Weber, F. Non-Newtonian Gravity in Strange Quark Stars and Constraints from the Observations of PSR J0740+6620 and GW170817. *Astrophys. J.* **2020**, *902*, 32. [CrossRef]
87. Banks, H.; McCullough, M. Charting the fifth force landscape. *Phys. Rev. D* **2021**, *103*, 075018. [CrossRef]

Disclaimer/Publisher's Note: The statements, opinions and data contained in all publications are solely those of the individual author(s) and contributor(s) and not of MDPI and/or the editor(s). MDPI and/or the editor(s) disclaim responsibility for any injury to people or property resulting from any ideas, methods, instructions or products referred to in the content.